

CHROM. 12,236

PREPARATIVE LIQUID CHROMATOGRAPHY: SAMPLE VOLUME OVERLOAD

B. COQ, G. CRETIER and J. L. ROCCA

E.R.A. 474, Laboratoire de Chimie Analytique III (Prof. M. Porthault), Université Claude Bernard Lyon I, 43 Bd. du 11 Novembre 1918, 69621 Villeurbanne (France)

SUMMARY

The maximal injection volume equation has been developed from the well-known expression for the output profile resulting from large sample input volume in elution chromatography. The validity of this equation is examined experimentally. In order to quantify the maximal sample load under volume overload conditions, the maximal injection concentration in the maximal injection volume is studied in terms of column dimensions and chromatographic parameters.

A sampling valve connected with a solute sprinkler is used with a split-stream technique and is compared with other injection modes with respect to band spreading and column loadability.

INTRODUCTION

For any chromatographic system, there is a maximal sample load; for a larger injection load, resolution between chromatographic peaks becomes inadequate. In order to work out a preparative-scale separation, determination of maximal sample load parameters is very important. For such a determination, the study of band broadening due to column overload is necessary.

Calculation of band broadening is simple when the column is overloaded by means of a large sample volume, *i.e.* the injection concentration is kept so that the column continues to operate in the linear part of the solute isotherm; in this case, band broadening only depends on injection volume. On the contrary, if the column is overloaded by means of a large sample mass, *i.e.* if the sample concentration is kept so that column operates in the linear and non-linear parts of solute isotherm, band broadening is proportional to injection volume and sample concentration; it further depends on isotherm shape¹. In this last case, any general discussion cannot be undertaken because the isotherm is a characteristic for a definite substance.

This work only deals with column volume overload and the column thus is assumed to operate in the linear part of solute isotherm. Maximal sample load, $Q_{i,\max}$, depends on two terms; maximal injection volume, $V_{i,\max}$, and maximal injection concentration in this volume, $C_{i,\max}$,

$$Q_{i,\max} = C_{i,\max} V_{i,\max} \quad (1)$$

If the input function is a square wave and the column acts as a Gaussian operator, the solute profile is described by the well-known relationship²:

$$C = \frac{C_i}{2} \left[\operatorname{erf} \left(\frac{V - V_R}{\sqrt{2}\sigma} \right) - \operatorname{erf} \left(\frac{V - V_R - V_i}{\sqrt{2}\sigma} \right) \right] \quad (2)$$

C is the solute concentration at output volume V ; C_i the sample concentration in the feed solution; V_R the retention volume; V_i the injected volume and σ the standard deviation of the Gaussian peak.

According to Reilley *et al.*² and if the injected volume V_i is large enough ($V_i > 8\sigma$), it is easy to demonstrate that the peak width at the base ΔV is given by:

$$\Delta V = V_i + 2.5\sigma \quad (3)$$

Thus, under volume overload conditions, the band broadening ΔV versus injected volume V_i plot is linear.

Resolution R_S between two solutes 1 and 2 can be written:

$$R_S = \frac{V_{R2} - V_{R1}}{V_i + 1.25(\sigma_1 + \sigma_2)} \quad (4)$$

The 1 and 2 indexes refer to the first and second eluted solutes, respectively.

Recovery of products with a definite purity needs a minimum resolution $R_{S,\min}$ for which the injection volume becomes maximum $V_{i,\max}$:

$$V_{i,\max} = V_0 \left[\frac{k'_1(\alpha - 1)}{R_{S,\min}} - \frac{1.25}{\sqrt{N}} (2 + k'_1 + \alpha k'_1) \right] \quad (5)$$

k'_1 is the capacity factor of the first eluted solute; α , the selectivity factor; V_0 the column dead volume and N the theoretical plate number which is supposed not to depend on solute retention.

The maximum injection volume depends on chromatographic parameters (k'_1 , α and N) and is directly proportional to column dead volume V_0 .

The first part of this work deals with the experimental examination of the $V_{i,\max}$ expression in terms of chromatographic parameters and column dimensions. In order to determine the maximum injection load under volume overload conditions, it is also necessary to study the variations of the maximum injection concentration $C_{i,\max}$ (in the maximum injection volume, $V_{i,\max}$), and the maximum injection concentration is further studied empirically in terms of capacity factor k'_1 and column dimensions.

Eqn. 5 supposes a square wave input function; that is applicable for very large injection volumes because the contribution of the injection mode to the deformation of the output profile can be considered to be negligible; if the injected volume decreases, this approximation is no longer valid and it is necessary for the injection mode to deliver input profiles as perfectly square as possible. The second part of this paper deals with comparison of different injection modes with respect to band spreading and column loadability.

EXPERIMENTAL

Materials and apparatus

In all experiments, the mobile phases were binary mixtures of *n*-heptane and ethyl acetate. The solvents were of high purity and supplied by SDS (Peypin, France) and Rhône-Alpes Chimie (Caluire, France). The solutes used were some phthalates: diheptyl phthalate (DHP), di-isobutyl phthalate (DIBP), dibutyl phthalate (DBP) and diethyl phthalate (DEP).

Three sets of chromatographic equipment were used:

System I: chromatograph Chromatospac Prep 10 (Jobin Yvon, Longjumeau, France) connected with the variable wavelength UV detector Jobin Yvon Monospac 103 (80 mm³ cell volume).

System II: chromatograph Miniprep LC (Jobin Yvon) connected with the same detector.

System III: this system was assembled from the following elements: the reciprocating pumps of the 3520 chromatograph Spectra Physics (Spectra Physics, Palaiseau, France), the VALCO Model CV-6-UHP sampling valve (Sopares, Gentilly, France) the ISCO Model UA-4 UV detector (Roucaire, Velizy, France) or the differential refractometer Waters Model R 401 (Waters, Paris, France).

All columns were slurry packed either by the technique required for a particular column (longitudinal compression, Jobin Yvon's columns) or by the classical method³, in one step for the 25 cm × 10 mm I.D. column and in four steps for the 25 cm × 20 mm I.D. column.

The stationary phases used were silica gel H60 (10–40 μm), LiChroprep Si 60 (15–25 μm) (Merck, Paris, France) and Partisil 5 (6 μm) (Whatman, Ferrières, France).

Procedures

In order to avoid any dispersion effect of the sample due to the parabolic velocity profile in the external loop and to deliver a square wave⁴, the loop volume was twice the injection volume: the sample was injected into the column by allowing the mobile phase to flow through the sample loop for a given time which was determined from the flow-rate and volume of sample selected for injection, and then the valve was rotated to allow the mobile phase to pass directly into the column.

For injection of large volumes, the chromatographic system III was used consisting of one pump for elution and the other for injection (Fig. 1). The two pumps were set at the same flow-rate D . The first pump supplied the mobile phase to the column, the second supplied the sample solution to an adjustable constriction (c). The flow-rate was adjusted to the value D with a pressure drop identical to that of the column. This is necessary to avoid any variation in flow-rate when the pump is functioning in the injection mode. During the time period $t_i = V_i/D$, injection of V_i was carried out by connecting the pump to the column by means of rotation of the 6-way valve. After the time period t_i , the valve was reset to its original position in which the column was again fed by the elution pump.

The effect of the method of sample introduction was studied with four injection modes (Fig. 2): in all four modes, a sampling valve was used with different column-top terminators.

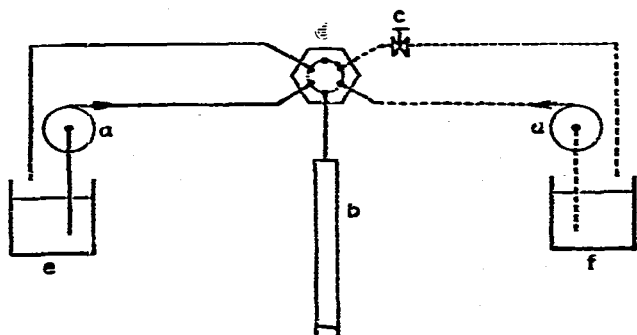


Fig. 1. Injection device for large sample volume. a = Pump, b = 6-way valve, c = adjustable constriction, d = column, e = solvent tank, f = sample tank. ···, Injection phase; —, elution phase.

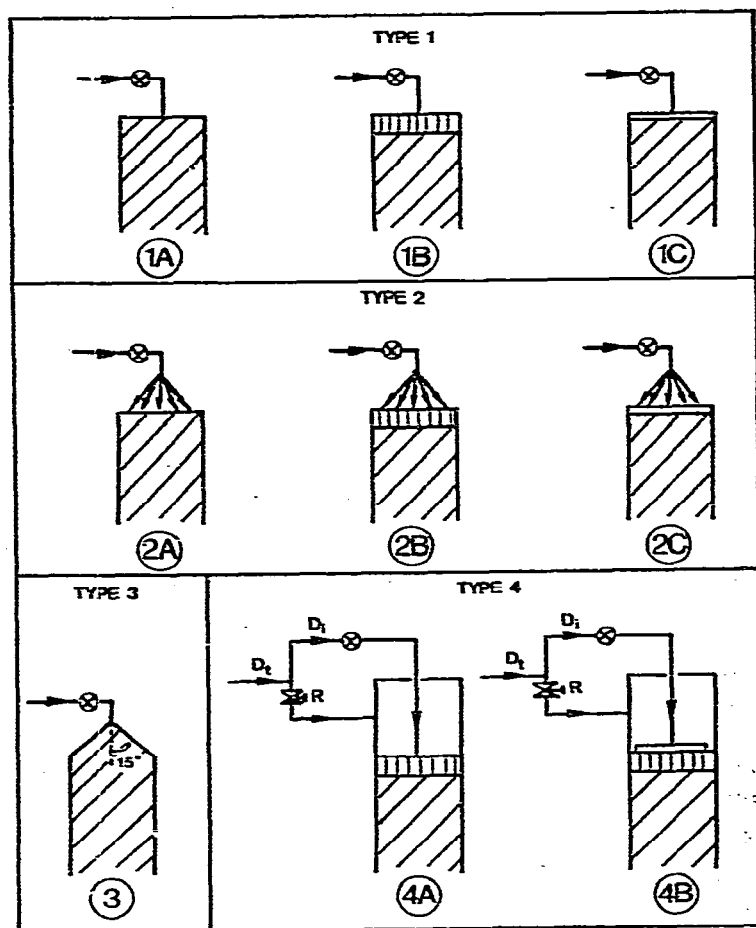


Fig. 2. Schematic representation of the injection devices used. ⊗ = sampling valve, ⊠ = stainless-steel frit, □ = dead volume.

With the first type of injection system, the injection valve was directly connected with the column and the sample was introduced at one point on the cross-section of the column with a 0.5 mm I.D. tube.

With the second type of injection system, the sample was introduced at five points on the cross-section of the column⁵ by means of a group of 0.5 mm I.D. tubes — one at the center surrounded by the four others at regular intervals on a 14 mm diameter circle.

For the third type of injection system, a conical column top filled with stationary phase was installed between the column packing and the injection valve.

For the fourth type of injection system, the injection valve was used with a split-stream technique⁶⁻¹⁰. The principle of this technique is to divide the flow (total flow-rate D_t) into two parts: one towards the injection valve (flow-rate D_i) and the other directly to the column (flow-rate $D_t - D_i$) through a metering valve which enables adjustment of the ratio D_i/D_t . The 4A injector was comparable with on-flow syringe injection in that there was continuous elution flow forcing the injection plug to move in certain flow lines away from the wall. With the 4B injector, the split-stream system was combined with a dual-purpose sprinkler. This sprinkler provides widespread distribution of the sample over the column packing, thus decreasing the risk of local overload. The sample arriving from the injection valve through the central tube flows out through 10 small 0.3 mm diameter holes on the lower side of the sprinkler. Moreover the mobile phase was distributed over the cross-section of the column by means of three large 2 mm I.D. tubes through the sprinkler (Fig. 3).

In order to improve the radial dispersion of the sample, a 2 mm thick stainless steel frit, 100 times more permeable than the column packing, was used on the column-top for the 1B and 2B injection systems¹¹ and a small dead volume, 0.5 mm deep was used for the 1C and 2C injection systems.

For these experiments, the 25 cm \times 20 mm I.D. column was used with a bottom terminator allowing the eluate to be recovered on the entire section of the column (Fig. 4). Band broadening of the elution peak was characterized by means of the variance calculated from moment analysis.

The quality of the separation between two adjacent peaks 1 and 2 was followed by means of either the recovery ratio of the first solute r_1 when its collection was stopped at the valley between the two peak or the purity of the second component P_2 when it was totally collected:

$$r_1 = \frac{Q_{i,1} - m_1}{Q_{i,1}} \quad (6)$$

$$P_2 = \frac{Q_{i,2}}{Q_{i,2} + m'_1} \quad (7)$$

where $Q_{i,1}$ and $Q_{i,2}$ are the injected amounts of the solutes 1 and 2, respectively, m_1 is the non-collected amount of the solute 1 by stopping the collection at the valley, and m'_1 is the collected amount of the solute 1 by collection of the whole injected amount of the solute 2.

For m_1 determination, the column eluate was collected from the valley between the two peaks and its solute 1 content was analysed quantitatively with external calibration. For the m'_1 determination, the overlapping middle portion between the

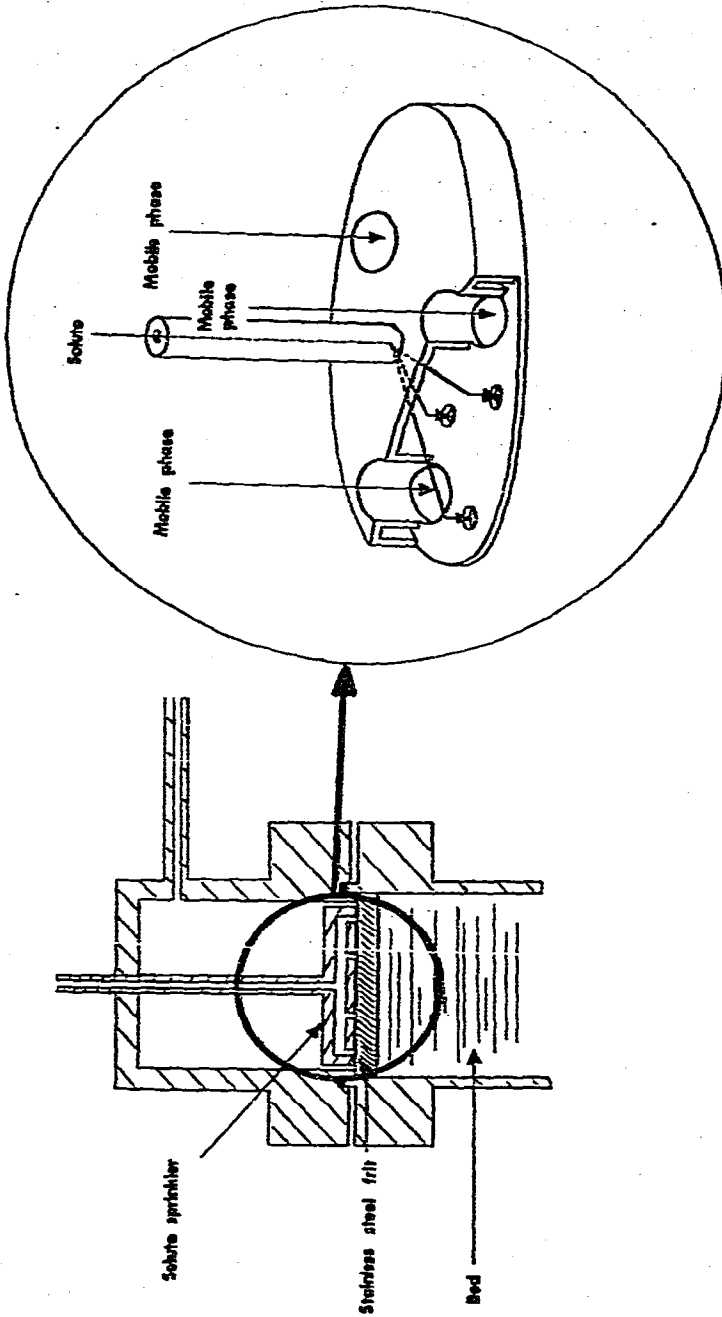


Fig. 3. Detailed representation of the 4B injector.

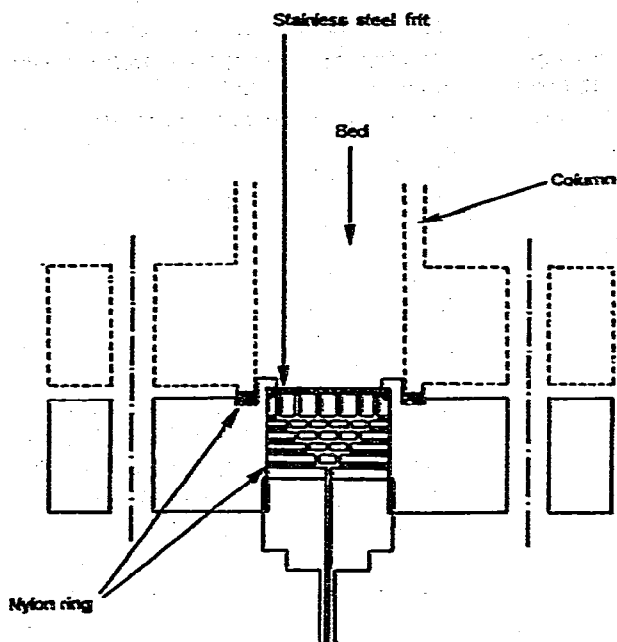


Fig. 4. Schematic representation of the column-bottom terminator.

two peaks was fractionated and the solute I content of each fraction was analysed quantitatively with internal calibration with diheptyl phthalate as internal standard. r_1 and P_2 were equal to 100% when the two solutes were separated without any peak overlap.

RESULTS AND DISCUSSION

Maximum sample load

The experimental examination of the validity of the maximum injection volume (eqn. 5) and the study of the maximum injection concentration in the maximum injection volume in terms of column characteristics and chromatographic parameters are performed with chromatographic conditions given in Tables I and II.

TABLE I

COLUMNS AND CHROMATOGRAPHIC APPARATUS USED FOR THE STUDY OF THE MAXIMUM INJECTION LOAD WITH REGARD TO COLUMN CHARACTERISTICS

Stationary phase: LiChroprep Si 60, 15–25 μm ; mobile phase: *n*-heptane–ethyl acetate (80:20, v/v); solutes: DBP ($k' = 0.13$), DEP ($k' = 0.56$); $\alpha = 4.3$.

Chromatographic apparatus	Column			
	Flow-rate (cm^3/min)	Length, L (cm)	Inner diameter d_c (cm)	N
I	15	15	4	1500
	15	30	4	3200
II	4	20	2	2200

TABLE II

CHROMATOGRAPHIC SYSTEMS USED FOR THE STUDY OF MAXIMUM INJECTION WITH REGARD TO CHROMATOGRAPHIC PARAMETERS

Column: 25×1.04 cm I.D.; $N = 10000$; flow-rate: $3 \text{ cm}^3/\text{min}$; chromatographic apparatus I.

Stationary phase	Mobile phase	Solute	k'_i	α
Partisil 5 6-7 μm	<i>n</i> -Heptane-ethyl acetate (85:15)	DBP	0.56	2.44
		DEP	1.37	
	<i>n</i> -Heptane-ethyl acetate (90:10)	DBP	0.96	2.30
		DEP	2.21	
	<i>n</i> -Heptane-ethyl acetate (97:3)	DBP	4.80	2.08
		DEP	9.98	

The first set of experiments deals with the influence of the column dead volume V_0 on the maximum injection volume $V_{i,\text{max}}$. With columns of various lengths and inner diameters (Table I), the theoretical values of $V_{i,\text{max}}$ are calculated according to eqn. 5 with $R_{s,\text{minl}} = 0.95$ and these volumes are injected onto the columns. The measurements of DEP purity P_{DEP} are given in Table III; all purity values are nearly identical and equal to 100%; they demonstrate that, whatever the geometric characteristics of the column, the experimental maximum feed volume can be calculated from eqn. 5. Moreover, these results illustrate that with such large injection volumes (from 21 up to 150 cm^3), deformation originating from the injection device is negligible and the input function can be considered as a square wave.

In the second set of experiments, the influence of chromatographic parameters (capacity factor k'_i and selectivity factor α) on $V_{i,\text{max}}$ is studied. Chromatographic conditions are summarized in Table II. In a similar manner, the maximum injection volume is calculated from eqn. 5 with $R_{s,\text{minl}} = 1$ and this volume is injected into the three different chromatographic systems. The dibutyl phthalate recovery ratios r_{DBP} obtained are given in Table IV. As in the preceding study, the constancy of the separation quality characterized by r_{DBP} confirms the validity of eqn. 5 in predicting the maximum injection volume $V_{i,\text{max}}$ with respect to k'_i and α .

TABLE III

INJECTION OF CALCULATED MAXIMAL VOLUME, $V_{i,\text{max}}$, AND VARIATIONS OF DEP PURITY, P_{DEP} , WITH COLUMN CHARACTERISTICS

Length (cm)	I.D. (cm)	N	V_0 (cm^3)	$V_{i,\text{max}}$ (cm^3)	P_{DEP} (%)
20	2	2200	54	21	98.7
15	4	1500	185	70	98.9
30	4	3200	375	150	99.1

TABLE IV

INJECTION OF CALCULATED MAXIMUM VOLUME, $V_{i,\text{max}}$, AND VARIATIONS OF DBP RECOVERY RATIO, r_{DBP} , WITH CHROMATOGRAPHIC PARAMETERS

k'_i	α	$V_{i,\text{max}}$ (cm^3)	C_i (mg/cm^3)	r_{DBP} (%)
0.56	2.44	11	20	98.8
0.96	2.30	17	10	99.1
4.80	2.08	70	2	99.0

When volume overloading occurs, the maximum injection volume is well defined by eqn. 5. The determination of the maximum injection load $Q_{i,max}$ (eqn. 1) needs the knowledge of the maximum injection concentration $C_{i,max}$. Therefore $C_{i,max}$ is studied experimentally in terms of column dimensions and capacity factor. For $C_{i,max}$ determination, the theoretical injection volume is calculated from eqn. 5, and sample concentration in this maximum injection volume is increased. The maximum injection concentration is reached when the peak undergoes an additional broadening and the separation quality decreases.

In Fig. 5, the diethyl phthalate purity P_{DEP} is plotted versus the sample concentration C_i for three different columns; the injected sample volume is the maximum injection volume calculated from eqn. 5 with $R_{S,mini} = 0.95$. The maximum injection concentration which is reached as soon as the quality of the separation decreases, is 5 mg/cm³; from this figure it appears that $C_{i,max}$ does not depend on the column dimensions. So, it is seen from eqns. 1 and 5 that, under volume overload conditions, maximum sample load is directly proportional to column dead volume; it does not depend on the geometry of the column provided that the column volume is kept constant.

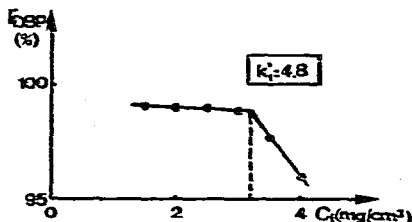
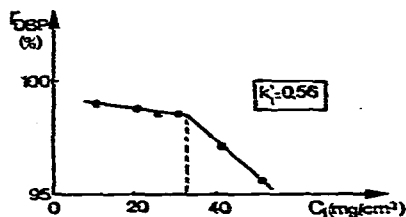
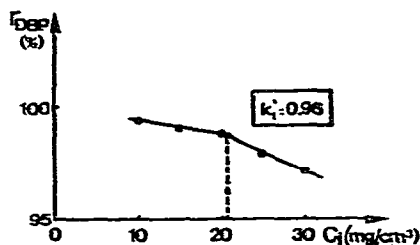
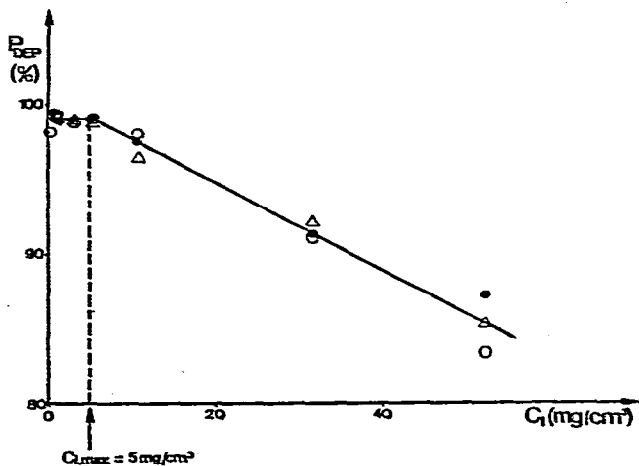


Fig. 5. Plot of P_{DEP} versus sample concentration C_i for three different columns. \circ , 20 \times 2 cm I.D.; \bullet , 15 \times 4 cm I.D.; \triangle , 30 \times 4 cm I.D. Conditions as in Table I.

Fig. 6. Plots of r_{DEP} versus sample concentration C_i for three different chromatographic systems. Conditions as in Table II.

The plots of the dibutyl phthalate recovery ratio r_{DBP} versus the sample concentration C_1 shown in Fig. 6 correspond to three different chromatographic systems (see conditions in Table II); in each case, the injection volume is maximum and calculated from eqn. 5 with $R_{S,\text{minl}} = 1$. Table V summarizes the maximum injection concentrations $C_{i,\text{max}}$ and the maximum injection loads $Q_{i,\text{max}}$ under volume overload conditions. The maximum injection concentration $C_{i,\text{max}}$ decreases while the capacity factor k'_1 increases but the product $C_{i,\text{max}} \cdot k'_1$ remains roughly constant: it can be concluded that $C_{i,\text{max}}$ is directly proportional to $1/k'_1$.

TABLE V

VARIATIONS OF MAXIMUM INJECTION CONCENTRATION, $C_{i,\text{max}}$, WITH CAPACITY FACTOR, k'_1

Parameter	k'_1		
	0.56	0.96	4.80
α	2.44	2.30	2.08
$V_{i,\text{max}}$ (cm ³)	11	17	70
$C_{i,\text{max}}$ (mg/cm ³)	34	20.5	3.5
$Q_{i,\text{max}} = C_{i,\text{max}} V_{i,\text{max}}$ (mg)	374	349	245
$C_{i,\text{max}} k'_1$	19.0	19.7	17.8

When chromatographic parameters are such that the terms $k'_1 \cdot (\alpha - 1)$ or N are large enough, the expression of the maximum injection volume is

$$V_{i,\text{max}} = V_0 k'_1 \frac{\alpha - 1}{R_{S,\text{minl}}} \quad (8)$$

and the maximum injection load is given by

$$Q_{i,\text{max}} = C_{i,\text{max}} k'_1 \frac{V_0 (\alpha - 1)}{R_{S,\text{minl}}} \quad (9)$$

it follows that under such conditions, the maximum injection load does not depend on capacity factor k'_1 because $C_{i,\text{max}} \cdot k'_1$ is constant for any k'_1 value.

$$Q_{i,\text{max}} = A V_0 \frac{\alpha - 1}{R_{S,\text{minl}}} \quad (10)$$

and $Q_{i,\text{max}}$ only depends on one chromatographic parameter: the selectivity factor.

In our experiments, the terms $k'_1 \cdot (\alpha - 1)$ or N were not large enough and $Q_{i,\text{max}}$ is not independent of the capacity factor and decreases with increasing k'_1 (Table V).

Comparison of different injection devices

In analytical chromatography and in preparative chromatography as well, an ideal injection device must deliver a square wave input function into the head of the column, to minimise contribution of the injection to band broadening. This condition

was fulfilled in the preceding part of this work when the injected volumes were large enough to allow the deformation resulting from the injection process to be neglected with respect to the large sample volumes.

In some cases, when the injection volume decreases, the input function is no longer assimilated with a plug, and it is necessary to improve the injection technique. Furthermore, in preparative chromatography, this technique must allow a solute repartition in order to decrease the injected amount of solute per unit area and to minimise the band broadening resulting from local overload of the stationary phase in the upper part of the column. The four injection devices tested here are given in Fig. 2. For their comparison, the resolution between two phthalates (DHP and DIBP) is followed with a 1.5 cm³ injected volume and 1.5 mg injected amount of each phthalate. The quality of the separation is characterized by means of recovery ratio for DHP (r_{DHP}). The experimental values with each injection device are summarized in Table VI. All inlet devices with the sampling valve directly connected to the column, give bad results. In that case, an uneven flow profile arises in the column extremity and the peak undergoes hydrodynamic deformation¹¹; the resolution between the two phthalates is bad due to large peak tailing (Fig. 7a). Better peak symmetry is obtained when the sampling valve is used with a split-stream technique (Fig. 7b): with these systems (the so-called split-stream injectors), quasi stagnant eluent areas are avoided and the sample is injected into a non-disturbed flow pattern which prevents any hydrodynamic deformation^{10,11}; the resolution between the two phthalates and the diheptyl phthalate recovery ratio are good. These improvements of peak symmetry and column efficiency on using the injection valve with a split-stream technique, were already noticed by some workers⁶⁻¹⁰ but a solute sprinkler which allows feeding of the mobile phase on the entire column section and solute repartition, was never used.

TABLE VI

DHP RECOVERY RATIO, r_{DHP} , OBTAINED WITH DIFFERENT INJECTION DEVICES

Chromatographic system III; Wavelength: 254 nm; 25 × 2.1 cm I.D. column; stationary phase: silica gel H60 (10–40 μm); mobile phase: *n*-heptane–ethyl acetate (90:10, v/v); flow-rate: 10 cm³/min; solutes: DHP ($k' = 0.6$), DIBP ($k' = 1.13$); sample volume: 1.5 cm³; sample concentration of each solute: 1 mg/cm³.

Injection device	r_{DHP} (%)
1A	87.2
1B	87.4
1C	89.5
2A	87.5
2B	87.9
2C	85.5
3	83.3
4A	99.6
4B	98.9

Use of split-stream injectors demands a preliminary adjustment of the ratio D_i/D_t (D_i is the flow-rate in the injection valve and D_t is the total flow-rate). Peak variance σ_t^2 (Fig. 8) and elution peak shape (Fig. 9) depend on this ratio D_i/D_t . From the σ_t^2 versus D_i/D_t plot, the optimal flow-rate ratio $(D_i/D_t)_{opt}$ can be found with

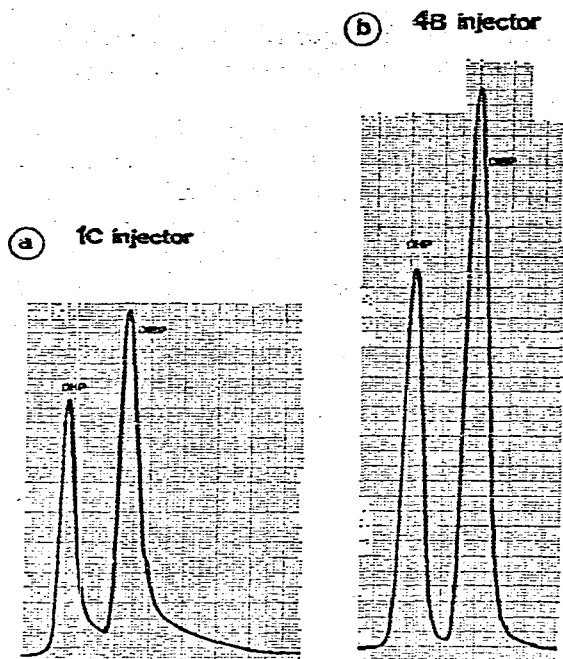


Fig. 7. Chromatograms demonstrating peak shape obtained with 1C and 4B injectors. Experimental conditions, see Table VI. (a) 1C injection device; (b) 4B injection device.

which variance is minimal. Moreover, this optimal ratio allows the peak to be symmetric (Fig. 9b); larger values lead to peak tailing similar to that obtained with the injection valve directly connected with the column (Fig. 9a). This band deformation

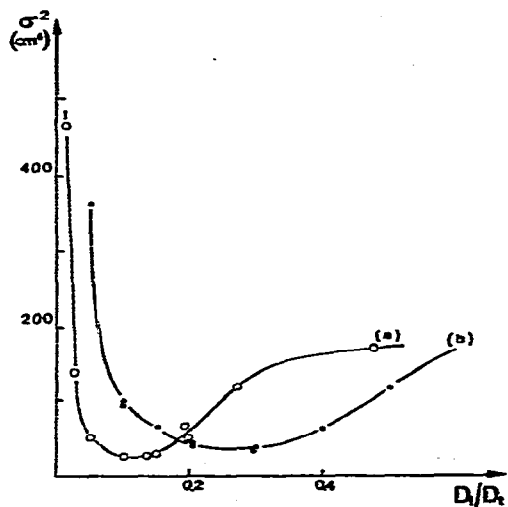


Fig. 8. Plots of total variance σ_t^2 versus flow-rate ratio D_1/D_t for (a) 4A injector and (b) 4B injector. Experimental conditions, see Table VI.

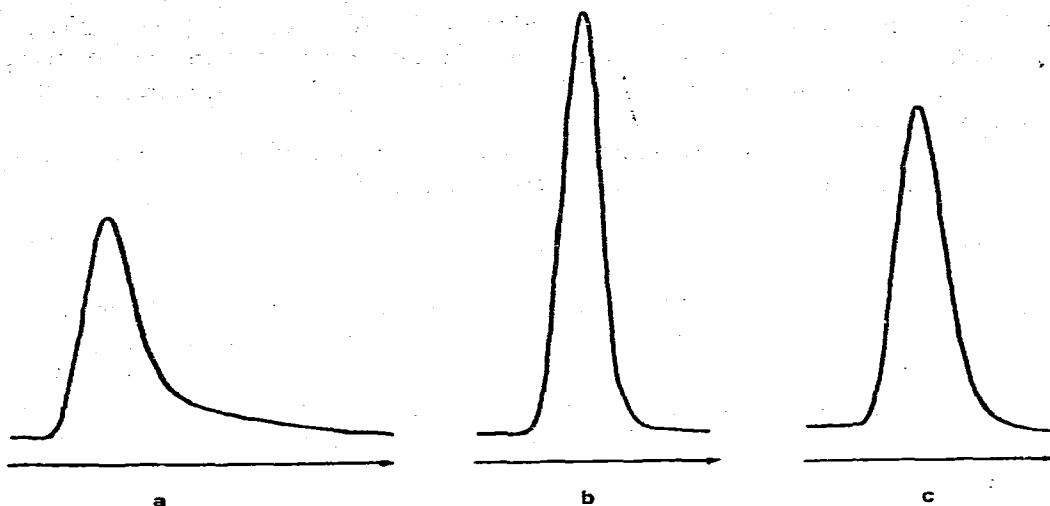


Fig. 9. Chromatograms demonstrating influence of the flow-rate ratio D_i/D_r on peak shape. (a) $D_i/D_r = 0.60$, (b) $D_i/D_r = 0.25$ (optimal ratio), (c) $D_i/D_r = 0.01$. Experimental conditions, see Table VI. 4B injection device.

probably results from the uneven flow field set up in the column extremity and is assumed not to depend on injected volume V_i . For lower value, the chromatographic peaks are symmetric but much more widened (Fig. 9c); this peak broadening results from too long an injection time, that is proportional to V_i . So in adjusting the optimal flow-rate ratio these two opposite phenomena must be taken into account, and plotting of this ratio *versus* the injected volume becomes necessary; the experimental values are shown in Fig. 10. According to the preceding comments, $(D_i/D_r)_{opt}$ increases with increasing V_i . For large V_i values, the $(D_i/D_r)_{opt}$ values are the same with the two split-stream injectors because the V_i term mainly contributes to band spreading.

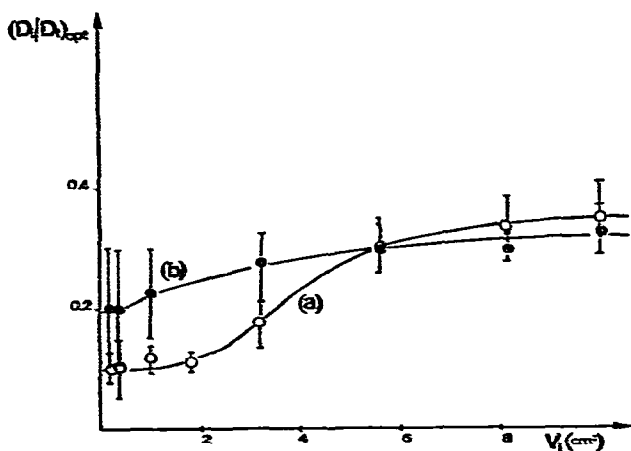


Fig. 10. Plots of optimal flow-rate ratio $(D_i/D_r)_{opt}$ versus sample volume V_i for (a) 4A injector and (b) 4B injector. Experimental conditions, see Table VI.

On the contrary, for small V_i values, the adjustments are lower with the 4A injector than with the 4B one. Undoubtedly these results must be related to the flow pattern, the prevalent factor in band spreading; for a definite (D_i/D_c) value it depends on the geometric characteristics of the two injectors.

Some workers¹²⁻¹⁴ considered the standard deviation of the injection profile, σ_i , to be directly proportional to the injection volume V_i :

$$\sigma_i = \psi V_i \quad (11)$$

where ψ is a parameter which characterizes the injection method. Clearly, the smaller the ψ value, the better the injection device. For plug injection, ψ is equal to $1/\sqrt{12} \approx 0.29$. If other extra column effects than the injection effect can be assumed to contribute little to band broadening, the total volume variance σ_t^2 measured on the chromatogram is the sum of the injection variance σ_i^2 and the column variance σ^2 :

$$\sigma_t^2 = \psi^2 V_i^2 + \sigma^2 \quad (12)$$

Thus, the σ_t^2 versus V_i^2 plot will allow the determination of ψ . Figs. 11 and 12 show this plot, respectively, with the 1A injector and the split-stream injectors (for each injected volume $(D_i/D_c)_{opt}$ is chosen according to Fig. 10). ψ is equal to 0.75 with the two split-stream injectors and 0.37 with the 1A one. However, the peak variance is smaller with the split-stream injectors, *i.e.* their contribution to band broadening is smaller. The lower value of band spreading with the split-stream injectors seems to be in contradiction to their ψ -factors. In fact, splitting of the flow-rate involves dilution of the sample so that the true injected volume is more precisely described by

$$V_i' = \frac{V_i}{D_i/D_c} \quad (13)$$

The factor ψ' between the standard deviation of the injected band, σ_i , and the injection volume V_i' is equal to 0.26 (Fig. 13). This value which slightly differs from $1/\sqrt{12}$,

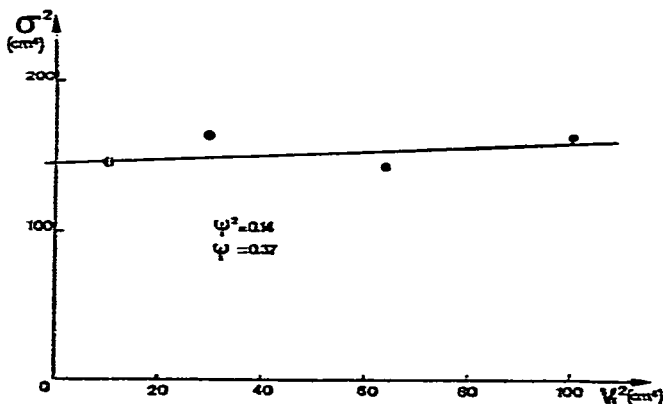


Fig. 11. Plot of total variance σ_t^2 versus square sample volume V_i^2 for the 1A injector. Experimental conditions, see Table VI.

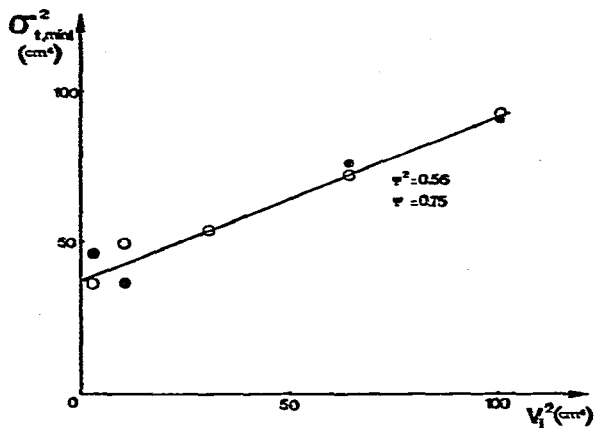


Fig. 12. Plot of minimal total variance $\sigma_{t,\min}^2$ versus square sample volume V_i^2 for the two split-stream injectors. O, 4A injector; ●, 4B injector. Experimental conditions, see Table VI.

means that with the split stream injectors, a square wave is introduced onto the column. The width of the plug is $V_i(D_i/D_t)$.

Moreover, in preparative liquid chromatography, it is also important to pay attention to the distribution of the sample over the entire column section so that local overload of the stationary phase is decreased. To study this effect, the sample concentration in the two split-stream injectors is increased, with a constant 3.16 cm^3 injection volume; Fig. 14 illustrates the effect on the separation quality between DHP and DIBP (characterized by r_{DHP}). With the 4A injector, solute repartition does not exist because the sample is injected at one point of the packing and the stationary phase is overloaded as soon as the sample concentration reaches 3 mg/cm^3 ; with the 4B injector, the sprinkler allows the solute to be spread out over the cross-section of the column and the stationary phase overload only occurs from 100 mg/cm^3 onward.

Use of the split-stream 4B injector makes it possible to inject large sample volumes and large sample concentrations onto large diameter columns; this injection

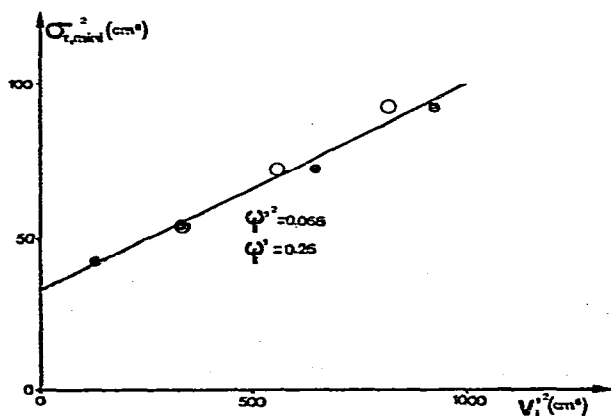


Fig. 13. Plot of minimal total variance $\sigma_{t,\min}^2$ versus square apparent injected volume $V_i'^2$ for the two split-stream injectors. Experimental conditions, see Table VI.

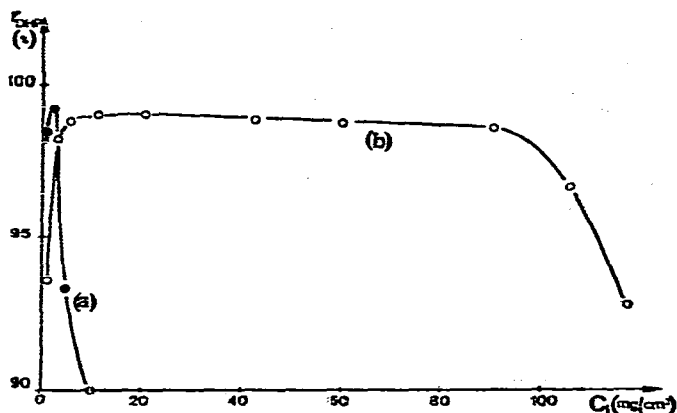


Fig. 14. Plot of r_{DUR} versus sample concentration C_i for the two split-stream injectors. (a) 4A injector, $(D_i/D_t)_{opt} = 0.18$; (b) 4B injector, $(D_i/D_t)_{opt} = 0.28$. Sample volume: 3.16 cm^3 . Other conditions, see Table VI.

mode prevents the chromatographic peak from any hydrodynamic deformation and local overload of the stationary phase then results from larger sample loads.

Among the injection devices tested, the split-stream technique seems to be the only injection mode for delivering square wave inputs. But the sample dilution occurring with the splitting of the flow-rate (eqn. 13), limits injection of large sample volumes and the maximum injection volume (eqn. 5) becomes

$$V_{i,max} = V_0 \frac{D_t}{D_i} \left[\frac{k'_1(\alpha - 1)}{R_{S,mini}} - \frac{1.25}{\sqrt{N}} (2 + k'_1 + \alpha k'_1) \right] \quad (14)$$

However, because of this dilution phenomenon, the sample concentration inside the column, C'_i , is given by

$$C'_i = C_i \frac{D_t}{D_i} \quad (15)$$

where C_i is the sample concentration in the feed solution. Then the maximum sample load $Q_{i,max}$ (eqns. 1, 14 and 15) no longer depends on the D_i/D_t term. The preceding experimental results agree with this assumption, however, further experiments are needed.

CONCLUSIONS

The maximal injection volume is simply calculated when the column is operating in the linear part of solute isotherm. This maximal injection volume is proportional to column dead volume, solute retention, selectivity factor and theoretical plate number; it further depends on injector quality and minimum resolution to achieve sufficient solute separation.

Under volume overload conditions, sample loading will be maximum when solute concentration in the maximum injection volume is also maximum. The maxi-

imum injection concentration does not depend on column dimensions; it is inversely proportional to the capacity factor of the first eluted solute. Therefore, the maximum sample load does not depend on this capacity factor if the chromatographic system is selective enough.

The method of sample introduction significantly influences the column loadability. The sampling valve used with a split-stream technique makes it possible to inject any sample volume onto large diameter columns without any hydrodynamic deformation of the injection plug.

Moreover, when a solute sprinkler is used, the column loadability is largely increased. The column could be used under volume overloading conditions, with the relevant theoretical expression.

REFERENCES

- 1 G. Cretier, *Thesis*, Lyon, 1979.
- 2 C. N. Reilly, G. P. Hildebrand and J. W. Ashley Jr., *Anal. Chem.*, 34 (1962) 1198.
- 3 B. Coq, C. Gonnet and J. L. Rocca, *J. Chromatogr.*, 106 (1975) 249.
- 4 R. P. W. Scott and P. Kucera, *J. Chromatogr.*, 119 (1976) 467.
- 5 A. Wehrli, *Z. Anal. Chem.*, 277 (1975) 289.
- 6 T. J. N. Webber and E. H. McKerrell, *J. Chromatogr.*, 122 (1976) 243.
- 7 E. Godbille and P. Devaux, *J. Chromatogr.*, 122 (1976) 317.
- 8 J. J. Kirkland, W. W. Yau, H. J. Stoklosa and C. H. Dilks, *J. Chromatogr. Sci.*, 15 (1977) 303.
- 9 A. W. J. de Jong, H. Poppe and J. C. Kraak, *J. Chromatogr.*, 148 (1978) 127.
- 10 B. Coq, G. Cretier and J. L. Rocca, *Chromatographia*, 11 (1978) 461.
- 11 B. Coq, G. Cretier and J. L. Rocca, *Analisis*, 7 (1979) 339.
- 12 E. Glueckauf, *Trans. Faraday Soc.*, 51 (1955) 34.
- 13 J. F. K. Huber, J. A. R. J. Hulsmann and C. A. M. Meijers, *J. Chromatogr.*, 62 (1972) 79.
- 14 J. C. Stenberg, *Advan. Chromatogr.*, 2 (1966) 205.